Characterization of Electric Field-induced Fusion in Erythrocyte Ghost Membranes

ARTHUR E. SOWERS
American Red Cross Laboratories, Bethesda, Maryland 20814

ABSTRACT Fusion has been reported to occur in a variety of membrane systems in response to the application of certain electric currents to the medium (Zimmermann, U., 1982, *Biochim. Biophys. Acta.*, 694:227–277). The application of a weak but continuous alternating current causes the membranes in suspension to become rearranged into the "pearl-chain" formation. Fusion can then be induced by one or more strong direct current pulses that cause pore formation. This results in the conversion of individual membranes in the "pearl-chain" formation to a single membrane with one or more hourglass constrictions that form lumens which connect the cytoplasmic compartments. As the diameter of the lumens increases, the overall membrane shape grows to one large sphere. To further characterize electric field-induced fusion, experiments were conducted using the erythrocyte ghost as a model membrane, and a new combination of electrical circuit and fusion chamber that is simpler and improved over previous systems. All odd-shaped ghosts (collapsed or partly collapsed spherical shapes, echinocytes, discocytes, and stomatocytes) in 30 mM phosphate buffer was first converted to spherocytes and then fused with increasing yields by increasing the number of pulses. After fusion, the lateral diffusion of a fluorescent lipid soluble label (DiI) from labeled to unlabeled membranes was observed to occur both with and without the appearance in phase-contrast optics of distinct communication (lumens) between cytoplasmic compartments of the fused membranes. Connections between cytoplasmic compartments, however, were unmistakable with the instant transfer of a fluorescent water-soluble label (fluorescein isothiocyanate-dextran) from labeled to unlabeled cytoplasmic compartments upon fusion. Although pulses still resulted in the lateral diffusion of DiI to unlabeled membranes, the presence of glycerol in the medium strongly reduced the yield of lumens observable by phase-contrast optics in fusion events. The presence of glycerol also inhibited the conversion of membranes to spherocytes, but did not inhibit the lateral diffusion of DiI from labeled to unlabeled membranes.

Membrane fusion has been induced in many membrane systems using procedures involving electric fields (for extensive reviews, see references 1–4). In general, membranes in suspension are fused by first exposing the suspension to a lower strength alternating current (AC)[1] that causes the membranes to come close to each other as they line up in the so-called "pearl-chain" formation. This phenomenon has been named dielectrophoresis (5). Fusion is then induced by applying a higher strength direct current (DC) pulse. The mechanism of fusion presumably involves the formation of pores when the transmembrane voltage from the DC pulse exceeds the breakdown threshold for the membrane, and occurs when random collision of free hydrophobic edges of these pores in separate membranes results in membrane continuity.

The observable morphological changes after fusion are dramatic. Phase-contrast micrograph sequences start by showing two membrane entities in contact. After the fusion-inducing pulse, the two entities immediately become one hourglass-shaped membrane entity. The sequence continues by showing a progressive time-dependent increase in the diameter of the hourglass constriction, or lumen, that finally ends in a perfect or near-perfect sphere (see reference 2, Fig. 8).

[1] *Abbreviations used in this paper:* AC, alternating current; DC, direct current; DiI, fluorescent dye, 1,1′-dihexadecyl-3,3,3″,3′-tetra-methylindocarbocyanine perchlorate; FITC, fluorescein isothiocyanate.

THE JOURNAL OF CELL BIOLOGY · VOLUME 99 DECEMBER 1984 1989–1996

Membrane fusion and fusion-associated phenomena are of general interest due to their ubiquitous involvement in biological processes and our incomplete understanding of the mechanism of fusion; they are of special interest in terms of creating specific experimental conditions. These conditions may involve fusing membranes to mix membrane components having different origins or delivery of certain substances to a recipient cytoplasm or internal aqueous compartment. Measuring the lateral diffusion coefficient of mobile membrane components by fusing labeled and unlabeled membranes and observing the rate of mixing has been reported for several systems (6–8), and has been recently given the acronym FRAF (fluorescence redistribution after fusion) (8). All of these procedures involve fusion events that occur at various times after the fusion-inducing conditions are created. However, reports that fusion can be observed to take place instantly or nearly instantly after one or more fusion-inducing DC pulses offers the possibility of improving the fluorescence redistribution after fusion approach to measuring lateral diffusion in membranes. The purpose of this paper is to do the following: (*a*) characterize several previously unreported aspects of the nature of the membrane connection made during the fusion event in erythrocyte ghost membranes; (*b*) characterize several previously unreported fusion-influencing variables; and (*c*) describe an alternative electrode-fusion chamber system and an alternative electrical circuit for generating and applying AC and DC currents to the membrane fusion chamber. Portions of this work have been reported in preliminary form (9).

MATERIALS AND METHODS

Human whole blood collected in plastic bags that contained citrate-phosphate dextrose-adenine as anticoagulant was obtained from the Washington, DC American Red Cross Regional Blood Center. Packed erythrocytes were obtained by centrifugation at 300 *g* for 10 min, then washed at least once in isotonic sodium phosphate buffer (pH 7.4), hemolyzed in 5 mM sodium phosphate buffer, and washed and stored overnight in 20 mM sodium phosphate buffer as a pellet. All steps were carried out at 0–4°C and pH 8.5 unless otherwise indicated.

The next day, working membrane suspensions were made. To do this, ghost membranes were diluted to 1/10 pellet concentrations by adding 9 vol 30 mM sodium phosphate buffer.

Ghost membranes were labeled by adding 0.05 ml of a stock solution of the fluorescent dye 1,1′-dihexadecyl-3,3,3″,3′-tetra-methylindocarbocyanine perchlorate (DiI) (C_{16}) in ethanol (3.5 mg/ml) to 4.45 ml of ghost membrane suspension in the desired buffer. Excess dye was removed by one or two washes in buffer at the desired ionic strength. Membranes were dehydrated by washes in buffers that contained specified glycerol concentrations (vol/vol).

Ghost cytoplasmic compartments were labeled by adding 1.0 ml of a solution (1.5% wt/vol) and M_r 10,000 fluorescein isothiocyanate (FITC)-dextran in 20 mM phosphate buffer to 1.0 ml of a erythrocyte ghost pellet from erythrocytes freshly hemolysed at 0–4°C and washed as above, warming to room temperature for 2 h, and then washing twice with the desired buffer at room temperature. The final pellet was resuspended to a working suspension with 9 ml of the desired buffer at room temperature.

The fusion slide is illustrated in Fig. 1. Membrane fusion chambers were made from a microslide (~10 × 2 mm) cut with a diamond scribe from a standard 25 × 75 mm glass microscope slide and a standard #1 thickness (22 × 22 mm) standard microscope cover glass. The microslide and cover slip were attached to each other as shown with Parafilm using a dry mounting press or double stick tape (Fig. 1*A*). This assembly was, in turn, attached with tape to the fusion slide with the chamber positioned in the center of the rectangular well such that the two wire electrodes were positioned on each side of the microslide and between the strips of tape holding the microslide to the cover glass (Fig. 1*B*). The wire electrodes are made of solder-tinned #22 gauge copper hook-up wire. Enough membrane suspension was added to one side of the microslide to make a droplet which flooded the wire electrode and filled the chamber by capillary wicking. Continuity of the membrane suspension with the other electrode was completed by adding a droplet to the other side of the microslide such that it flooded the other electrode and coalesced with the suspension in the space between the microslide and cover glass. The whole assembly was inverted and placed on the microscope stage.

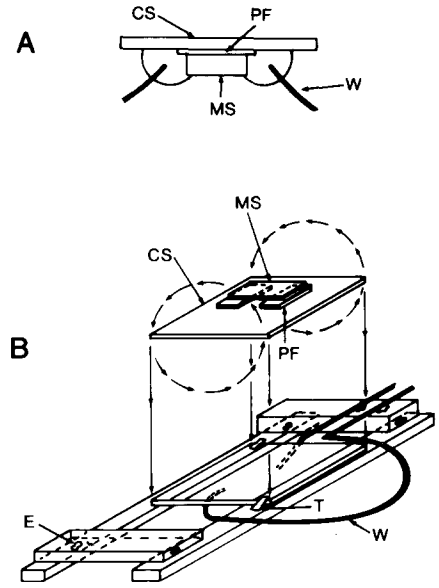

FIGURE 1 Fusion slide. (*A*) Fusion chamber made by heat sealing of a microslide (*MS*) with parafilm (*PF*) in a dry mounting press to a coverslip (*CS*); (*B*) fusion chamber, mounted with tape (*T*), in a frame made from glass strips cut from a standard microscope slide and cemented together with epoxy cement (*E*). Wire electrodes (*W*) are anchored to the frame with epoxy cement.

Electrical currents were fed to the wire electrodes using a circuit shown in Fig. 2. All AC used was from the secondary of an isolation transformer with a 1:1 turns ratio and fed with a variable (0-132 V) voltage transformer supplied with power from the 60 Hz AC power line. In accordance with previous reports of electric field-induced fusion, randomly distributed ghost membranes lined up in the pearl-chain formation in the fusion chamber with the membranes close to each other within 5–15 s after the application of the AC which generated a calculated field strength of 7–15 V/mm. Direct current pulses producing an electric field strength of 500 or 700 V/mm and decay half-times of 0.2, 0.6, or 1.2 ms were applied at the rate of 2/s after the pearl-chains were formed.

All DC used was from a variable-voltage (0–1,000 V) electrophoresis-type power supply. The chosen AC and DC voltages were applied to the input terminals of the circuit shown in Fig. 2. The rate of discharge of the capacitor, and therefore the decay rate of the pulse, was controlled independently of the dimensions of the fusion chamber and the electrical conductivity of the membrane suspension by a variable resistance connected parallel to the fusion chamber. The pulse voltage was monitored by sampling electrodes that were separate from the electrodes used to deliver current to the fusion medium. Using an operational amplifier, the samples of the pulse voltage signal were fed into the high impedance input of a differential amplifier. The pulse current was monitored by sampling the voltage drop across a resistor connected in series with the fusion chamber current. Both the voltage and current waveform were recorded on a storage screen oscilloscope. Pulse decay half-times were measured from traces on the oscilloscope screen.

All microscopy and micrography were conducted with phase-contrast optics on a Zeiss Model 16 microscope with an MC63 camera system. Illumination from a tungsten light source or a Zeiss Microflash III xenon strobe lamp was used for phase-contrast images; an epi 100 W Hg light source was used for fluorescence images. A Zeiss No. 487709 filter set was used for fluorescence. Kodak 2415 recording film (developed in HC110, dilution A) or Kodak VR1000 (developed in Unicolor K2 process) were used for recording the phase-contrast or fluorescence images, respectively.

The fluorescent lipid-soluble dye was obtained from Molecular Probes, Junction City, OR. All other reagents were obtained from Sigma Chemical Co., St. Louis, MO.

RESULTS

Oscilloscope traces showed that the pulse voltage ascended to the peak voltage within ~50 μs (Fig. 3). The pulse voltage

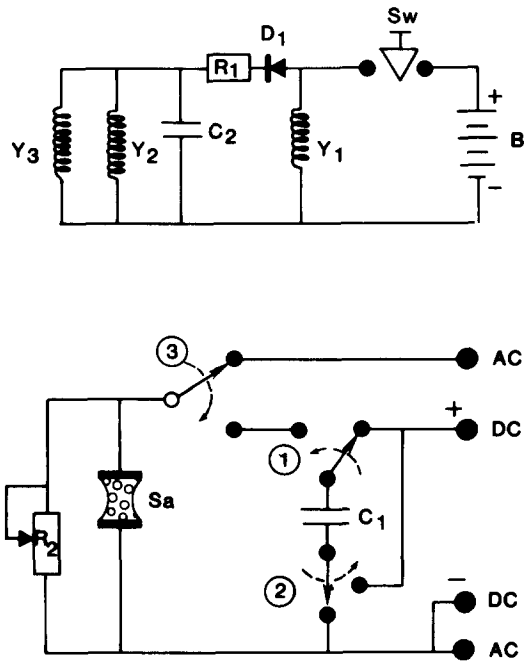

FIGURE 2 Electrical circuit used between an alternating current source (*AC*), a direct current source (*DC*), and the sample (*Sa*) membrane suspension contained within the fusion chamber. In this circuit, switch arms *1*, *2*, and *3* and normal positions of mercury-wetted relays (Clare Div., Chicago, IL [HGSM 5009, or equivalent]) are used to connect the *AC* or the *DC* to the sample. Capacitor C_1 is a 0.1-μF unit (Plastic Capacitors, Inc., Chicago, IL [Type OF50-104 or equivalent]). Variable auxillary load resistance (R_2) is a variable resistor covering the range 2,000–200,000Ω. Battery (*B*) is a 9-V transistor battery and provides the energy, upon pressing switch (*SW*), to activate relay electromagnets *Y1*, *Y2*, and *Y3* such that the switch arms (*1*, *2*, and *3*, respectively) are moved in the direction of the dashed arrows, with arm *1* moving ahead of *2* and *3* through a delay introduced by a 51Ω resistor (R_1), and a 500 μF capacitor (C_2) (Sprague Electric Co., North Adams, MA [type TVA 1315]). Any silicon diode (D_1) forces arm *1* to switch back to the starting position ahead of arms *2* and *3* when *SW* is released. Optional resistor R_3 (1 KΩ), located in shorting wire between arms *1* and *2*, prevents excessive currents from passing through relay contacts (arms *1* and *2*) following release of *SW* (not shown). All parts were obtained from Newark Electronics, Beltsville, MD.

then decayed to zero with an approximate half-time, depending on the auxillary load resistance and medium conductivity, from 0.2 to 1.2 ms. Pulse current followed the corresponding voltage waveform. The conductivity of the medium as derived from the voltage and the current waveform was estimated to be $\sim 2 \times 10^{-3}\ \Omega^{-1}\ mm^{-1}$ for the buffers used. If converted entirely to heat and undiminished by conductive cooling to the chamber walls, the maximum amount of energy deposited within the membrane suspension volume contained by the fusion chamber would cause a temperature rise in the fusion medium of no more than ~0.3°C per pulse. All other combinations yielded a lower temperature rise per pulse. Strips of test paper capable of indicating 0.5 pH unit or less dipped into the reservoir pool on each side of the fusion chamber showed no more than a 0.5 pH difference in pH even after extensive application (>100) of direct current pulses with the longest decay half-time available.

Ghost membranes suspended in 30 mM phosphate buffer generally had shapes including spheres, highly collapsed spheres, and odd shapes (echinocytes and stomatocytes). We observed that the positions of all membranes within the boundaries of the fusion chamber changed such that the pearl-chain formation was achieved shortly (10–15 s) after the application of the AC, regardless of the shape of those membranes. Increasing the number of the fusion-inducing DC pulses resulted in progressive changes in the shapes of all oddly shaped and variably collapsed spherical ghost membranes. These membranes became perfect spheres before fusion was observed (Fig. 4). Conversion of oddly shaped membranes to perfect spherical membranes always occurred before pulse-induced lumens could be seen. Membranes that were spherical before the pulses were applied also fused after the application of the pulse. Membranes closer to the spherical geometry required fewer consecutive pulses to become spheres than membranes that were more highly collapsed. Complete conversion of all membranes to spherocytes required the fewest number of pulses when the pulses had a decay half-time (optimum) resulting in the maximum fusion yield. More pulses were required when the decay half-time was longer or shorter than optimum. These results were independent of whether the DC pulses were delivered to the membrane suspension as fast as two per second, or as slow as one per 10 seconds (not shown).

The application of fusion-inducing pulses to membrane suspensions that contained both DiI-labeled and unlabeled membranes resulted in the time-dependent lateral diffusion of the fluorescence from the labeled to the unlabeled membranes, and resulted in the formation of a distinct lumen at the hourglass constriction (Fig. 5 *a*). However, in the presence of glycerol, the membranes exposed to the fusion-inducing pulses showed the movement of DiI from the labeled membrane to the unlabeled membrane but without the formation of an observable lumen at the hourglass constriction (Fig. 5 *b–e*).

Fusion-inducing pulses were applied to mixtures of resealed membranes having FITC-dextran–labeled cytoplasmic compartments and unlabeled membranes held in the pearl-chain formation. These pulses resulted in four distinct changes (Fig. 6): (*a*) Labeled cytoplasmic compartments became continuous with other unlabeled compartments as the fluorescence became completely and uniformly distributed in the other compartments immediately after the pulses were applied. Viewing the same membrane pearl-chains in phase-contrast optics showed the presence of visually distinct lumens in some fused membranes. (*b*) Some pearl-chains showed uniform

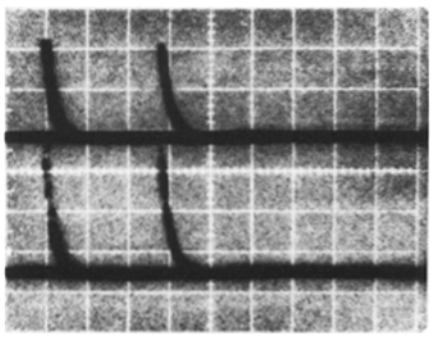

FIGURE 3 Recorded voltage pulse waveform (*bottom trace* 150 V per division) and associated current pulse waveform (*top trace* 5 × 10^{-4} A per division) using 30 mM buffer (pH 8.5) in the fusion slide chamber and a shunt resistance of 7 × 10^4Ω. Horizontal scale, 2.0 ms/div.

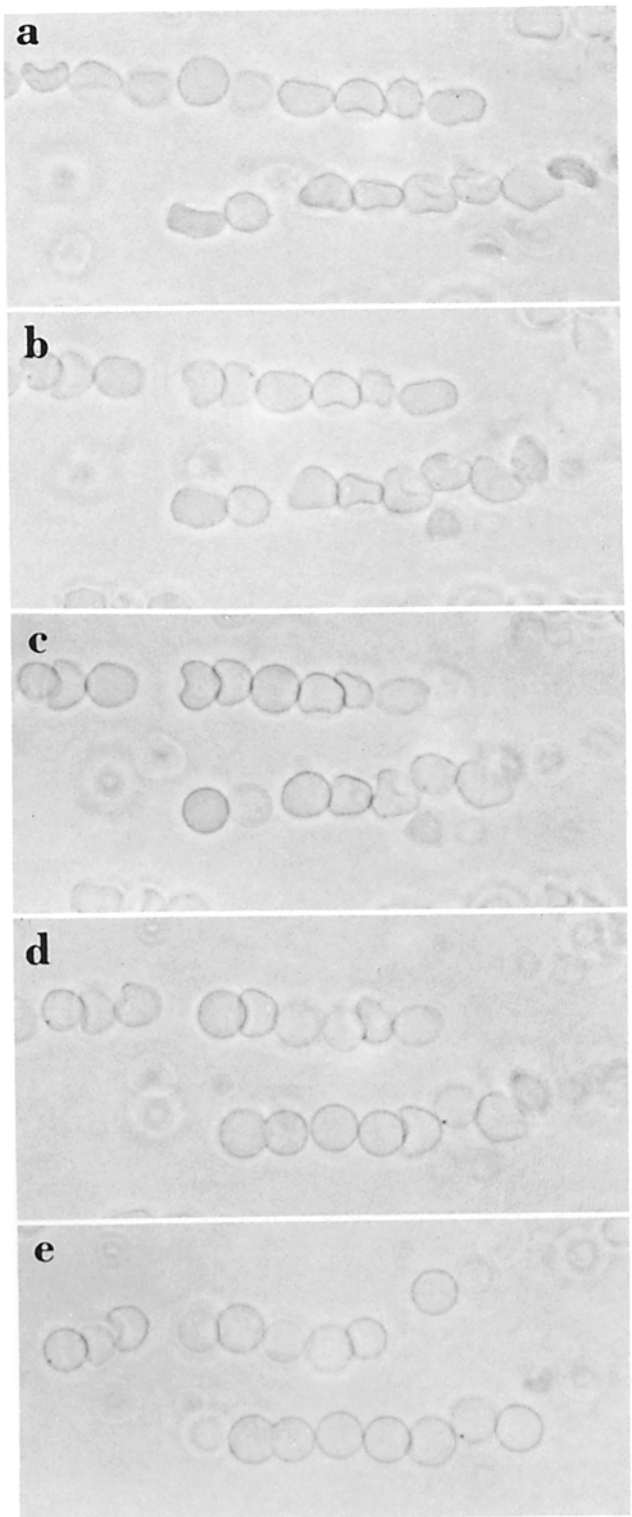

FIGURE 4 Observation by phase-contrast optics. Alignment into pearl chains and fusion of erythrocyte ghost membranes in 30 mM Pi buffer (pH 8.5). (a) Ghosts held in pearl chain formation. (*b*) Same ghosts 1.0 s after application of one fusion-inducing pulse (500 V/mm peak field strength, 0.2-ms decay half-time). (c) Same ghosts after a second pulse and 6 s after *a*. (*d*) Same ghosts after a third pulse and 8.5 s after *a*. (e) Same ghosts after two additional pulses (five total), and 13 s after *a*. Note progressive change of odd-shaped ghosts to perfect or near perfect spheres, single fusion event, and minor repositioning of membranes due to brownian motion. Photo width, 95 μm. × 830.

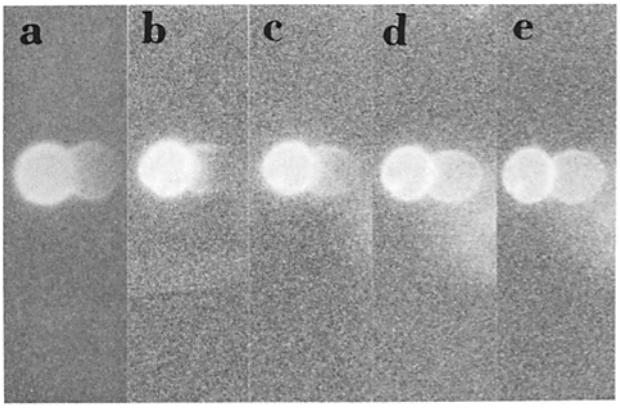

FIGURE 5 Observation by fluorescence of DiI. Movement of fluorescence from labeled membrane (left member) to unlabeled membrane (right member) following fusion events between membrane pairs. (a) Distinct lumen is visible at 19 s after fusion in 100% aqueous medium; (*b–e*) a distinct lumen is not visible at 7.5 (*b*), 19 (*c*), 35 (*d*), or 50 (*e*) s after fusion in 10% glycerol. Right member of pair starts sequence as an odd shape and ends sequence as a slightly elliptical shape. Photo widths, 20 μm. × 800.

fluorescence but no visually distinct lumen could be seen by phase-contrast optics. (*c*) Some pearl-chains did not show redistribution of the fluorescence to unlabeled compartments but evidently became attached to one another, since removal of the AC after the pulses were applied led to randomly oriented pearl-chains with fluorescence in only the originally labeled cytoplasmic compartments. (*d*) The fluorescence in some labeled cytoplasmic compartments moved to unlabeled cytoplasmic compartments only in steps that were discrete with, as well as simultaneous to, each applied pulse. A more uniform distribution of fluorescence was eventually observed with progressively more pulses. Using an electric field strength of 1,000 V/mm and a pulse decay half-time greater than 1.2 ms caused the fluorescence to disappear from the labeled cytoplasmic compartments and appear in the background.

Membranes dehydrated by glycerol permitted fusion to be observed between membranes that were not perfectly spherical (Fig. 5 *b–e*). This was the only time that fusion occurred before membranes became spherical upon application of fusion-inducing DC pulses.

We also observed that a reversal of the normal sequence of applying AC and then the DC fusion-inducing pulses could also result in fusion. In other words, the application of a given number of fusion-inducing pulses to randomly positioned membrane in the absence of the AC, followed immediately by the application of the AC, would result in fusion just as if the normal sequence (AC followed by DC pulses) was used.

An increase in glycerol concentration permitted fusion to occur among nonspherical membranes (Fig. 5 *b–e*). This is the only exception to our observation that both lumen and nonlumen production occurred only when membranes were first converted to the spherical shape as the fusion-inducing pulses were applied.

The fraction of all membranes in the pearl-chain formation that developed lumens visible by phase-contrast optics had a complex dependence on pulse decay half-time, number of pulses, and presence of glycerol (Fig. 7, top row). For the 100% aqueous medium, three to seven pulses and a decay

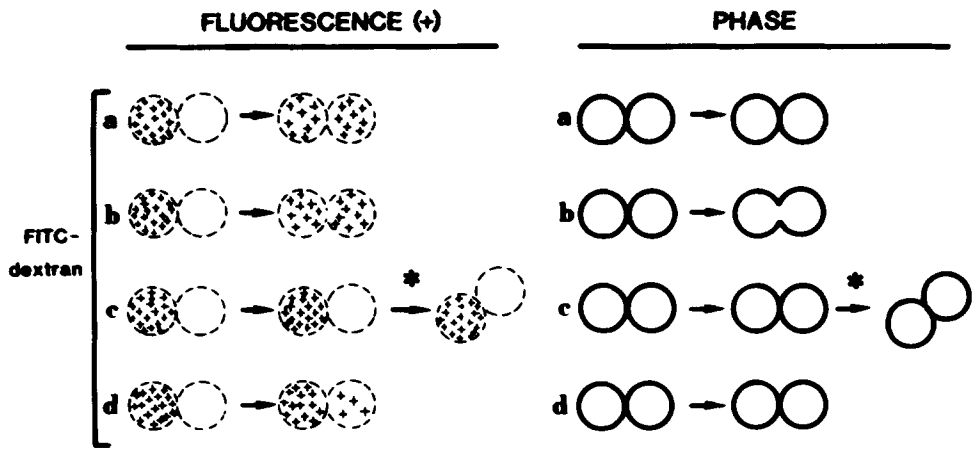

FIGURE 6 Summary of FITC-dextran-monitored and phase-contrast optics-monitored changes after the application of fusion-inducing pulses. (a) Movement of FITC-dextran from labeled cytoplasmic compartment to unlabeled cytoplasmic compartment to produce uniform labeling without formation of a lumen in phase-contrast optics. (*b*) Same as *a* except with the formation of a distinct lumen in phase-contrast optics. (*c*) No movement of label, however, physical membrane-membrane connection is indicated by random drift of cylindrical groups at some time after AC is removed (*). (*d*) Partial movement of label from labeled cytoplasmic compartment to unlabeled cytoplasmic compartment to produce a non-uniform labeling pattern in originally unlabeled cytoplasmic compartments.

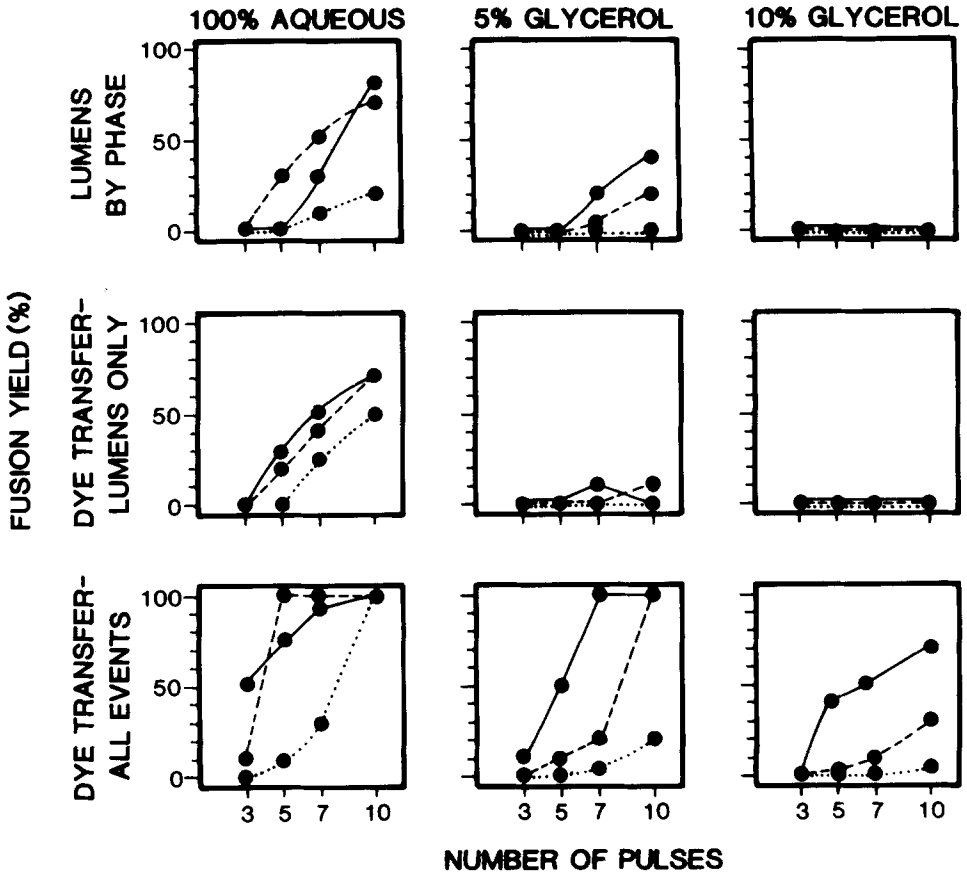

FIGURE 7 Fusion yield (%) as a function of *number of pulses*, pulse decay half-time (0.2 ms, dotted line; 0.6 ms, dashed; 1.2 ms, solid), and presence of glycerol (left column, 0% middle column, 5%; right column, 10%). *Top row*, fusion yield based on fraction of all membranes which develop distinct lumens as determined by phase-contrast optics (Fig. 4). *Middle row*, fusion yield based on fraction of all DiI-labeled membranes in which fluorescent label moves to at least one unlabeled membrane and is accompanied by a distinct lumen (Fig. 5*a*). *Bottom row*, fusion yield based on fraction of all labeled membranes in which fluorescent label moves to at least one unlabeled membrane regardless of whether it is accompanied by formation of a distinct lumen (Fig. 5, *b–e*). Peak electric field strength during pulse: 500 V/mm, *left column*; 700 V/mm, *middle* and *right columns*.

half-time of 0.6 ms resulted in the greatest yield. However, the greatest overall yield took place after 10 pulses with a decay half-time of 1.2 ms. Glycerol generally inhibited (5% glycerol) or eliminated (10% glycerol) the yield of lumens and shifted the pulse decay half-time for optimum yield from 0.6 to 1.2 ms.

The fraction of DiI-labeled membranes in which the label was passed to at least one originally unlabeled membrane was dramatically related to both the production of lumens and glycerol concentration. In general, glycerol almost completely inhibited lumen production (Fig. 7, middle row) but caused only a relatively small reduction in nonlumen-producing fusion yield (Fig. 7, bottom row). Addition of glycerol also shifts the pulse decay half-time for highest fusion yield from 0.6 to 1.2 ms. A peak electric field strength of 700 V/mm was used for both glycerol concentrations, and 500 V/mm was used for the 100% aqueous medium. This was because use of the higher field strength on membranes in the 100% aqueous medium caused both distortion of the membrane shape and lower yield, while use of the lower voltage in the glycerinated medium resulted in overall and proportionally lower yields (data not shown).

A subthreshold number of fusion-inducing pulses was applied to membranes that were held in the pearl-chain formation by the AC before removal of the AC and a short (1–2 min) wait. This resulted in randomly oriented membranes and randomly oriented cylindrical groups of spheres with two or more membranes each (Fig. 6).

Fusion yields were reproducible within experimental error if duplicate experiments were done with membranes from the same blood donor. Donor variability can result in a fusion yield variation of up to 15% in either direction.

DISCUSSION

The fusion slide and circuit used to obtain fusion in erythrocyte ghost membranes had advantages over previously described systems (*1–4*). The fusion slide is simple, inexpensive, and it contains disposable elements and electrodes which can be easily changed by desoldering and soldering. It permits electric field effects to be observed at a considerably greater (1–2 mm) distance from the electrodes where electrochemical and electrolytic processes may take place. It can be calculated (10) that, at the highest observed three-dimensional translational diffusion coefficients for solution components, a relatively large amount of time (many minutes) is needed before diffusion of electrolysis or electrochemical products from the electrode will arrive at the center of the fusion chamber. This procedure allows the use of the commonly available utility power lines as a convenient source of the AC needed to bring about the pearl-chain alignment of membranes.

The application of fusion-inducing pulses to a suspension of membranes in the pearl-chain formation results in the appearance of a lumen visually detectable by phase-contrast optics only if it is ~2 μm or greaer in diameter and increases in diameter with time (Fig. 4).

Fusion yield, in terms of both lumen-producing and nonlumen-producing events, is critically dependent on the pulse number, the pulse decay rate, and membrane hydration. Pulse decay half-times 0.2–1.2 ms are significantly longer than previously published optimum pulse lengths (1–4). Although the previously used pulse waveforms were claimed to be square (compared to the exponentially decaying waveform used in this study), actual oscilloscope traces were never published. Hence, the waveform as well as membrane hydration, pulse voltage, pulse number, and pulse length or decay rate may be very important in inducing fusion with electric field treatments. An analysis of the quantitative interdependence of these variables has also not been previously published.

Although examples exist in which the time-dependent increase in the diameter of some lumens falls short of achieving a final large spherical fusion product, the stability of the image indicates that fusion has occurred. Since the appearance of a lumen, however, satisfies the requirements (11, 12) for both cytoplasmic communication and membrane continuity, both membrane events can be designated as fusion. This is consistent with previous reports, and all previous reports of electric field-induced fusion have used this type of visual evidence for fusion (1–4). However, the time-dependent and irreversible lateral diffusion of DiI into adjacent unlabeled membranes, and the diffusion of FITC-dextran into adjacent unlabeled cytoplasmic compartments, respectively, demonstrated that membrane-membrane continuity can be produced in some of these electric field-induced membrane fusion events without producing a lumen detectable by either phase-contrast or fluorescence imaging of DiI-labeled membranes. The fact that nonlumen-yielding fusion events account for at least a small but finite fraction and, at most, a large and significant fraction of all fusion events, indicates that use of phase-contrast optics alone may significantly underestimate the fusion yield. Furthemore, nonlumen-producing fusion has important implications for our understanding of fusion phenomenology and cytoskeleton-related stabilization of membrane mechanical properties since the difference between nonlumen and lumen producing fusion events appears to be related to the stability of the connection made between membranes upon fusion.

Although bleaching of FITC-dextran fluorescence prevented photographic documentation and hindered visual scoring of phenomena observed over many minutes, several important observations were made. Two kinds of movement of FITC-dextran were observed in membrane fusion events that did not result in visually discernible outlines of membrane lumens by either phase-contrast optics or by the fluorescent membrane label. In the first kind of movement, the fluorescence moved rapidly, completely, and simultaneously with a single pulse to form a chain of polyspheres, all with equal brightness. In the second kind of movement, the first pulse caused a chain of fluorescent spheres to appear; one sphere (the sphere that originally contained the label) was much brighter than the others, and the others were uniformly dim. Successive pulses resulted in successively less difference in the fluorescence intensity between the bright sphere and the dim spheres until all spheres showed uniform fluorescence. It is obvious that the first kind of movement was due to the formation of a relatively large and permanent pore or lumen or a transient pore or lumen with a relatively long half-life (e.g., hundreds of ms). In the second kind of movement, the fluorescence moved rapidly but in discrete portions or increments that were simultaneous (within the limits of human reaction time) with each of several applied pulses. This kind of movement indicates that reversible transient connections between cytoplasmic compartments are formed only during passage of the current pulse through the membrane suspension. Conversely, the pore or lumen must be small enough or short-lived enough to prevent substantial equilibration of the concentration of the label among the originally labeled and originally unlabeled cytoplasmic compartments. The presence of distinct lumens by phase-contrast optics in fused membranes that showed uniform fluorescence was, of course, an obvious observation. On the other hand, an occasional cylinder of spheres adhering to one another was observed that

still showed fluorescence in only one of the membranes in the cylinder after several fusion-inducing pulses were delivered to the suspension. The reason that these few membranes were resistant to fusion is unknown. However, removal of the AC after the pulses were delivered resulted in the drift of cylindrical groups of spheres away from the parallel formation and towards a random distribution of membranes; this indicates that the pulses caused some sort of molecular rearrangement of the membrane that resulted in the membranes becoming attached to each other without (*a*) breaking or permeabilizing the membrane (no FITC-dextran loss from the cytoplasmic compartment to the suspension medium), (*b*) causing a fusion-related connection of labeled with unlabeled membranes (no lateral diffusion of DiI), or (*c*) causing cytoplasmic communication (FITC-dextran movement into unlabeled cytoplasmic compartments). Since the adhering spheres remain in a cylindrical form indefinitely, it may be possible that the glycocalyx and an intact cytoskeletal system are involved. A totally fluid membrane would otherwise result in randomly clumped aggregates rather than linear arrays.

Using 1.5 pm^3/d (13) and 10,000 d (the average molecular weight for FITC-dextran), we calculate a molecular volume of 15 nm^3 and a molecular diameter of 3 nm. Hence, the transient connections between cytoplasmic compartments must have a lumen diameter >3 nm for FITC-dextran to move into unlabeled compartments, and close to 3 nm (or any value smaller) when the transient connection is resealed. It is significant that this figure is close to the 4-nm diameter calculated indirectly in previous measurements on electric field-induced pores in reversible membrane breakdown experiments (14). Moreover, it should be pointed out that nonlumen-containing cylindrical arrays of spheres that show uniform fluorescence in all member sphere cytoplasmic compartments after one or more pulses do not allow a conclusion to be made concerning the state of cytoplasmic connections (a stable open [d > 3 nm] or a stable resealed [d < 3 nm] state). Nevertheless, both the membrane continuity and the cytoplasmic communication criteria for fusion were demonstrated in membrane events both with and without a large (>2 μm), unmistakable lumen. Therefore, we propose to refer to the former as lumen-producing fusion and the latter as nonlumen-producing fusion. Since lumen-producing fusion could be strongly inhibited by glycerol in 30 mM phosphate buffer, it is possible that membrane hydration may play a role in the membrane event that causes a microscopic lumen to become unstable and develop into a macroscopic lumen in which the diameter increases in a time-dependent manner. Although a role for membrane hydration in artificially induced fusion events has been previously discussed (15), it is not well understood. In any case, the data indicate that lumen production is functionally separate from the process of fusion.

Lastly, both types of fusion can be observed if fusion-inducing pulses are applied to a suspension of membranes in the absence of AC and then, after a period of 1–3 min, are followed by the application of the AC bringing the membranes into the pearl-chain formation. This suggests that the pulses induce fusion by a mechanism that destabilizes the membrane. Also, this destabilized state has a comparatively long lifetime (minutes) compared to the time needed for fusion to occur (seconds or fractions of a second). To our knowledge, this is the first direct evidence that a metastable fusogenic membrane state can be induced with a nonchemical stimulus. However, previous observations indicate that (*a*) indirectly detected electric field-induced pores reseal slowly compared to the duration of the current pulse in reversible membrane breakdown experiments (14), and (*b*) the pulse-induced perturbation of the phospholipid headgroup conformation may have a lifetime of as much as several minutes (16). If the formation of pores in the membrane is part of the fusion mechanism, then they must be <3 nm in diameter because pulse voltages and decay time can be found that result in substantial fusion yields with little or no detectable loss of FITC-dextran from labeled cytoplasmic compartments in this variation of the electric field protocol for inducing fusion. Significant FITC-dextran leakage does not occur after the fusion-inducing pulses are applied, and Brownian motion-induced tumbling tends to interfere with the coaxial alignment of pores needed for fusion (see Fig. 17 in reference 2). This suggests that the fusion mechanism and factors involved in creating the metastable fusogenic state are not as simple as previously suggested (see 1–4).

Intact erythrocytes in isotonic phosphate buffer (pH 7.4) can be fused in the same chamber with the same electric pulse circuit described here (see preliminary report in reference 17) if a concentration of cells is used that results in a monolayer of cells in physical contact after the cells settle to the bottom of the fusion chamber and more pulses are used. A full report will appear elsewhere.

Lumens in lumen-producing fusion events are generally first noticeable by phase-contrast optics not sooner than 15–30 s after the end of a train of fusion-inducing pulses are applied to a suspension of membranes. Examining a large number of membranes for lumens by phase-contrast optics requires that relatively little time can be spent looking at individual membranes for the subtle change which shows up as a small lumen. Hence, large fusion yields were often not perceivable until as much as 45–90 s later. Fusion events could thus be taking place at any time during this interval and therefore not be simultaneous. On the other hand, the start of the movement of the DiI from labeled membranes to the unlabeled membranes could be observed as early as 5–10 s after the end of a train of pulses, and the degree of penetration of the label into the unlabeled membranes can be used to estimate, by back extrapolation, when the fusion events took place. The observation of instantaneous (within human reaction time) pulse-induced movement of the FITC-dextran from labeled cytoplasmic compartment to unlabeled cytoplasmic compartment, however, permits the lower limit for fusion simultaneity to be estimated. Taking the lag time for human perception into account, electric field-induced fusion can, in at least a fraction of the membranes present, be now stated to be simultaneous within 100–200 ms.

The expert technical assistance of Ms. Veena Kapoor is greatly appreciated.

Contribution No. 613 from the American Red Cross Blood Services Laboratories. Supported in part by Biomedical Research Grant No. 5 SO RR 05737.

Received for publication 6 February 1984, and in revised form 6 June 1984.

REFERENCES

1. Zimmermann, U., P. Scheurich, G. Pilwat, and R. Benz. 1981. Cells with manipulated functions: new perspectives for cell biology, medicine, and technology. *Angew. Chem. Int. Ed. Engl.* 20:325–344.
2. Zimmermann, U. 1982. Electric field-mediated fusion and related electrical phenomena.

Biochim. Biophys. Acta. 694:227–277.
3. Zimmermann, U., and J. Vienken. 1982. Electric field-induced cell-to-cell fusion. *J. Membr. Biol.* 67:165–182.
4. Zimmermann, U., G. Pilwat, and H. A. Pohl. 1982. Electric field-mediated cell fusion. *J. Biol. Phys.* 10:43–50.
5. Pohl, H. A. 1978. Dielectrophoresis. Cambridge University Press, Cambridge. 579 pp.
6. Fowler, V., and D. Branton. 1977. Lateral mobility of human erythrocyte integral membrane proteins. *Nature (Lond.).* 268:23–26.
7. Frye, L. D., and M. Edidin. 1970. The rapid intermixing of cell surface antigens after formation of mouse-human heterokaryons. *J. Cell Sci.* 7:319–335.
8. Schindler, M., D. E. Koppel, and M. P. Sheetz. 1980. Modulation of membrane protein lateral mobility by polyphosphates and polyamines. *Proc. Natl. Acad. Sci. USA.* 77:1457–1461.
9. Sowers, A. E. 1983. Red cell and red cell ghost membrane shape changes accompanying the application of electric fields for inducing fusion. *J. Cell Biol.* 97(5, Pt. 2):178a. (Abstr.)
10. Sowers, A. E. 1983. Fusion of mitochondrial inner membranes by electric fields produces inside-out vesicles: visualization by freeze-fracture electron microscopy. *Biochim. Biophys. Acta.* 735:426–428.
11. Krutton, S., and C. A. Pasternak. 1979. The mechanism of cell-cell fusion. *Trends Biochem. Sci.* 4:220–223.
12. Gingell, D., and L. Ginsberg. 1978. Problems in the physical interpretation of membrane interaction and fusion. *In* Membrane Fusion. G. Poste and G. Nicolson, editors. Elsevier/North Holland Biomedical Press, Amsterdam. 791–833.
13. Henderson, R., and P. N. T. Unwin. 1975. Three-dimensional model of purple membrane obtained by electron microscopy. *Nature (Lond.).* 257:28–32.
14. Benz, R., and U. Zimmermann. 1981. The resealing process of lipid bilayers after reversible electrical breakdown. *Biochim. Biophys. Acta.* 640:169–178.
15. Lucy, J. A. 1978. Mechanisms of chemically induced cell fusion. *In* Membrane fusion. G. Poste and G. Nicolson, editors. Elsevier/North Holland Biomedical Press, Amsterdam. 267–304.
16. Stulen, G. 1981. Electric field effects on lipid membrane structure. *Biochim. Biophys. Acta.* 640:621–627.
17. Sowers, A. E. 1984. The lateral diffusion of DiI from a labeled membrane to an unlabeled membrane following electric field induced fusion: a new quantitative technique. *Biophys. J.* 45(2, Pt. 2):331*a*. (Abstr.)